

Natural hazards susceptibility mapping in Kuala Lumpur, Malaysia: an assessment using remote sensing and geographic information system (GIS)

Samy Ismail Elmahdy & Mohamed Mohamed Mostafa

To cite this article: Samy Ismail Elmahdy & Mohamed Mohamed Mostafa (2013) Natural hazards susceptibility mapping in Kuala Lumpur, Malaysia: an assessment using remote sensing and geographic information system (GIS), *Geomatics, Natural Hazards and Risk*, 4:1, 71-91, DOI: [10.1080/19475705.2012.690782](https://doi.org/10.1080/19475705.2012.690782)

To link to this article: <https://doi.org/10.1080/19475705.2012.690782>



Copyright Taylor and Francis Group, LLC



Published online: 02 Jul 2012.



Submit your article to this journal [↗](#)



Article views: 4341



View related articles [↗](#)



Citing articles: 3 View citing articles [↗](#)

Natural hazards susceptibility mapping in Kuala Lumpur, Malaysia: an assessment using remote sensing and geographic information system (GIS)

SAMY ISMAIL ELMAHDY* AND MOHAMED MOHAMED MOSTAFA

Faculty of Engineering, Civil and Environmental Engineering Department, United Arab
Emirates University, P.O.BOX 17555, Al-Ain, United Arab Emirates

(Received 28 October 2011; in final form 1 May 2012)

Intensive geological fractures and their associated karst features in tropical regions are often associated with unpredictable environmental and geotechnical engineering problems. This requires precise modelling using modern techniques. A 20 m spatial resolution Digital Elevation Model (DEM), a Geographic Information System (GIS) and Weighted Spatial Probability Modelling (WSPM) were integrated to predict the occurrence of flooding, landslides, sinkholes and earth subsidence in Kuala Lumpur, Malaysia. Five essential thematic layers were extracted using set of automated algorithms and then they were weighted. Layers included were geological fractures, stream network, micro-depressions, slope and lithological contact. All these thematic layers were assigned weights according to their level of contributions to the occurrence of flooding, landslide, sinkholes and earth subsidence. The map demonstrated that areas having very high geohazard susceptibility show an area of 4.155 km² (8%), whereas the areas characterized by low susceptibility for the occurrence of geohazard is approximately 16.394 (31.5%) of total Kuala Lumpur area. The natural hazard probability model was validated by comparing its results with the published landslide locations and geophysical and geotechnical maps of Kuala Lumpur and the comparison showed strong agreement.

1. Introduction

Geologists, geomorphologists and geotechnical engineers are all aware of the role of geological fractures (faults, joints, fissures and bedding planes) in natural resource accumulation (Mah *et al.* 1995, Samy 2006). They are serving as they do as buried channels for underground water movement, increasing the chemical and mechanical weathering of rocks and contributing to the instability of both hillslopes and bedrocks (Xeidakis *et al.* 2004). Thus, they are closely associated with the landslides, sinkholes, building collapse and earth subsidence (Gue and Tan 2001, Xeidakis *et al.* 2004, Samy *et al.* 2010a).

Surface and subsurface geological fractures and their associated karst terrain features represent a challenge for environmental and geotechnical engineers. For example, a location for the Petronas Twin Towers and Kuala Lumpur Convocation

*Corresponding author. Email: samy903@yahoo.com

Centre (KLCC) has been shifted 50 m away from their proposed location to one entirely within the Kenny Hill Formation (meta-sediments) (Azam *et al.* 1996, Tan 1996). This is due to the geological fractures, sinkholes, cavities and karst features forming an irregular surface of limestone bedrock, described as the worst terrain in the world (Gue and Tan 2001, Xeidakis *et al.* 2004, Zabidi *et al.* 2006, Samy *et al.* 2010b). In addition to cavities and sinkholes in Kuala Lumpur Limestone bedrock, landslides and rockfall show unpredictable environmental and geotechnical engineering problems in the adjacent mountainous areas. For example, hill view building collapse, which killed seven people in Kuala Lumpur, was reported due to the intensive geological fractures, steep slope and buried stream networks forming insatiability of the bedrock (Chow *et al.* 1996a). Sinkholes and earth subsidence are features commonly associated with the dissolution zones, along fault zones and lithological contacts between Kuala Lumpur Limestone and Kenny Hill Formation (Tan 1987, Gue and Tan 2001).

This demonstrates the need for a cost and time effective tool to precisely map the terrain factors that contribute to the natural hazard and predict these events. The use of remote sensing permits the revealing and mapping of the most crucial factors that are associated with unpredictable environmental and geotechnical engineering problems such as flooding, landslides, sinkholes, earth subsidence and building collapse.

Occurrence of flooding, landslides, sinkholes and earth subsidence has been studied for many decades using aerial photo interpretation and geophysical survey, but integration of remote sensing and Geographic Information System (GIS) has rarely been applied for predicting the occurrence of sinkholes and earth subsidence in Kuala Lumpur city centre, Malaysia. Therefore, there is a need to specify weight of the most contributing parameters toward natural hazard in Kuala Lumpur using different remote sensing data.

Using an integration of remote sensing and GIS, sites of unpredicted occurrence of environmental geotechnical engineering problems have been predicted for the first time. By means of spatial data analysis and integration, the complex of environmental and geotechnical problems can be predicted and investigated.

In the current study, in addition to using reasonable thematic layers of the most important factors for the prediction of environmental problems, validation using archived data and geotechnical maps was performed to check the accuracy of the obtained map.

2. Study area

The study area is located in the central part of the western belt of the Malaysian peninsula, stretching from $101^{\circ} 45' 45''$ E and $101^{\circ} 35' 15''$ longitude to $2^{\circ} 58' 30''$ N and $3^{\circ} 14' 15''$ N latitude, with a total area of approximately 52 km^2 (figure 1(a)). The eastern and western bordering hills are composed of granite, while the southern bordering hills are made up by the Kenny Hill Formation. Approximately 40% of Kuala Lumpur is underlain by highly fractured limestone. The only outcrop of Kuala Lumpur limestone bedrock located in the Batu Caves, in the form of a cliff of about 213 m in height (Tan 1987). The limestone area and its adjacent mountainous area are drained by several major rivers and streams, running south from the mountainous areas towards Kuala Lumpur city centre (GSM 1995).

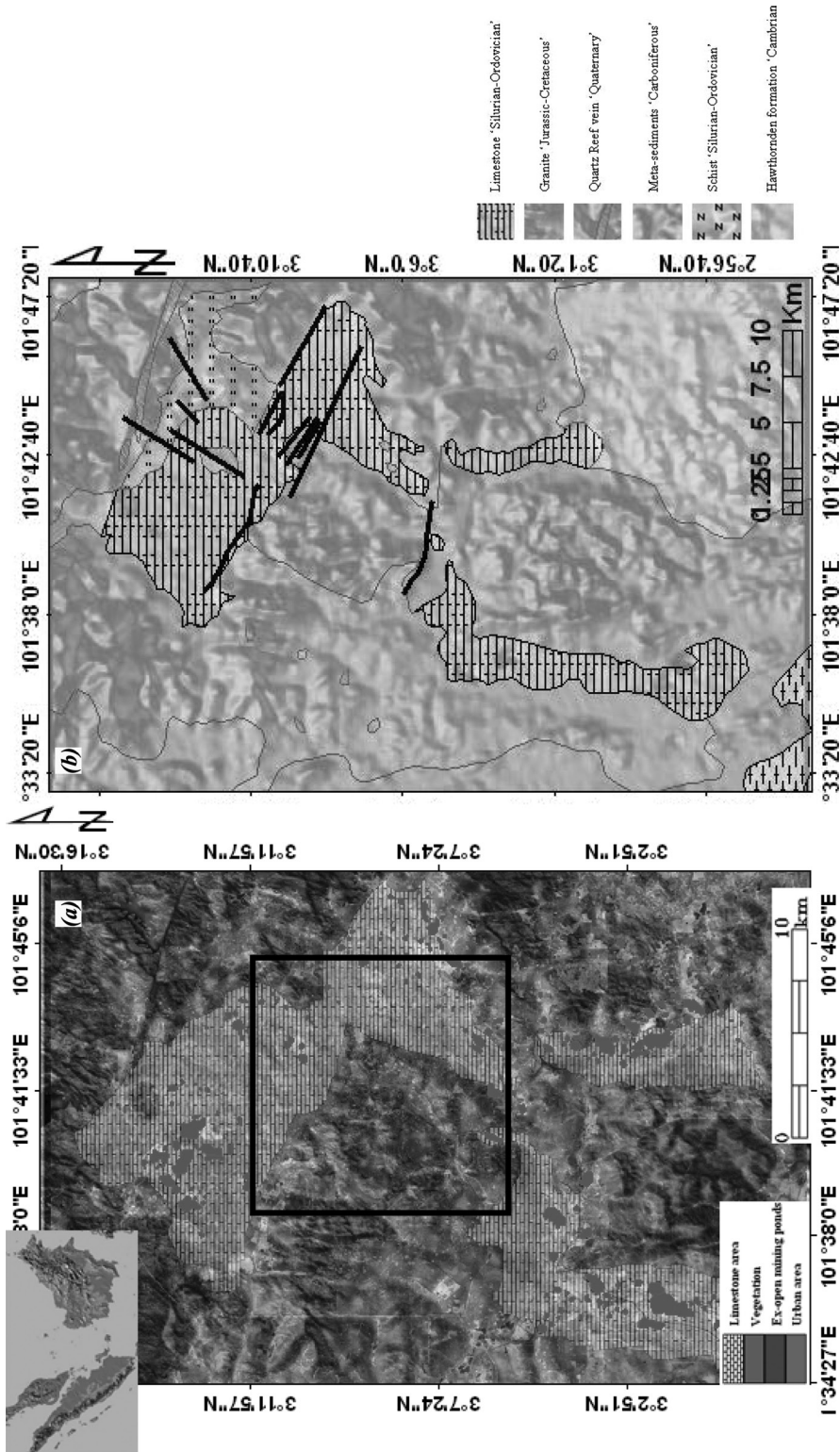


Figure 1. (a) LANDSAT ETM+ image and (b) geologic map of the study area showing the ex-open pit mining ponds, lithologic unites and fault zones. The black box highlights the Kuala Lumpur city centre.

The stratigraphic units consist of Hawthornden Formation (metamorphic rocks), Kuala Lumpur Limestone, Kenny Hill Formation and granite, and have experienced a series of tectonic events during geologic times. A tremendous number of geological fractures (Stauffer 1968, Yeap 1987) mark the eastern, western and southern boundaries. These geological fractures are tensional and wrench, with some low-lying both because of the regional shear stress that affects Kuala Lumpur and the successive tectonic events that occurred during the Silurian and Cretaceous periods (figure 1(b)). The orientations of the geological fractures are predominantly WNW–ESE, NNW–SSE and NE–SW (Gobbet 1964). The rainfall of the study area ranges from 300 mm to 400 mm during two distinct wet seasons from September to December and from February to May per annum as reported by the Drainage and irrigation department of Malaysia (figure 2; <http://www.met.gov.my>).

3. Material and methods

3.1 Data pre-processing

One of the most important steps in mapping was to construct an accurate Digital Elevation Model (DEM). In this instance, the traditional method of DEM and DTM

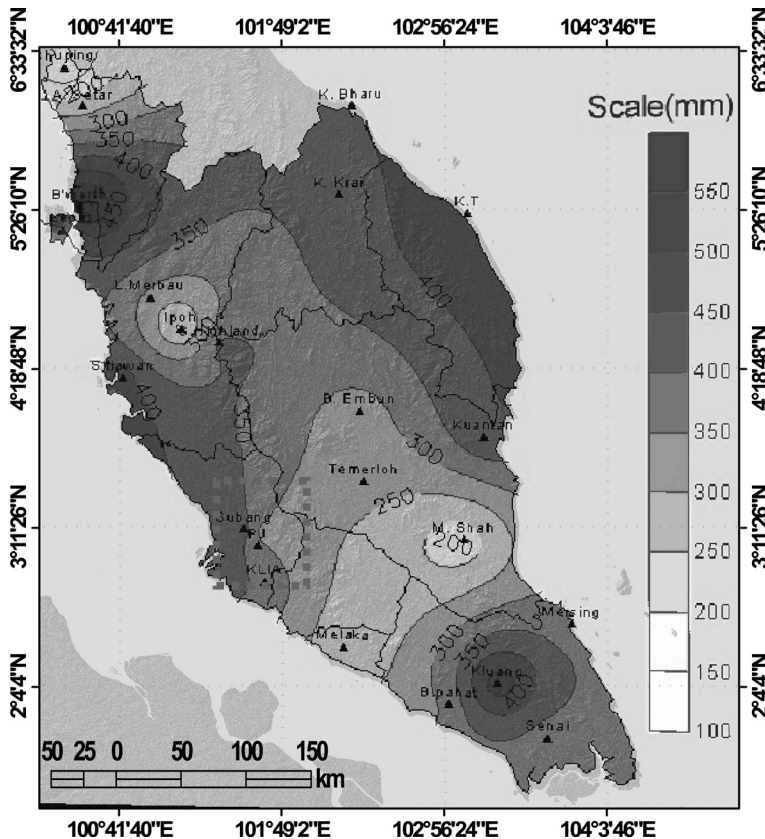


Figure 2. Rainfall distribution map for peninsular Malaysia. Red square highlights the location of investigated area (after <http://www.met.gov.my>). Available in colour online

generation from topographic maps and stereo-pairs would fail to construct a DEM of sufficient quality, due to the low slope and relief of the study area, while urban development could affect the accuracy and number of contour lines. To overcome this problem, two steps were applied to construct high quality of DEM. In the first step, the SRTM DEM of ~90 m spatial resolution was resampled to 30 m (<http://srtm.csi.cgiar.org/Index.asp>). The original cell size (0.000834 in decimal degrees) should be 0.000278 and the bilinear interpolation had higher accuracy and was quite effective. Then, the Z-factor of resampled STRM DEM was merged with the Z-factor of 30 m spatial resolution ASTER DEM (<http://www.gdem.aster.ersdac.or.jp/search.jsp>). In the second step, the new 30 m spatial resolution DEM and DTM generated from a 5 m contour interval topographic map were converted to contour lines. After that, the Z values of contour lines of DTM and DEM were merged to generate a more accurate DEM (figure 3).

To unify the scale of DEM with the geotechnical engineering map, the resultant DEM was then resampled to 20 m and enhanced by applying a local moving mean filter to reduce errors in the grid, such as artefacts or blunder errors, random errors or noise and systematic errors (Hengl *et al.* 2003).

3.2 Methods

3.2.1 Natural hazard susceptibility mapping. The indicators of natural hazard occurrence are related to geological fractures, stream network, micro-depressions, lithological contacts and slope of the area. In order to model and predict the natural hazard occurrence, different thematic maps (factors) were prepared. These include four different thematic maps as essential and crucial factors were integrated in the GIS

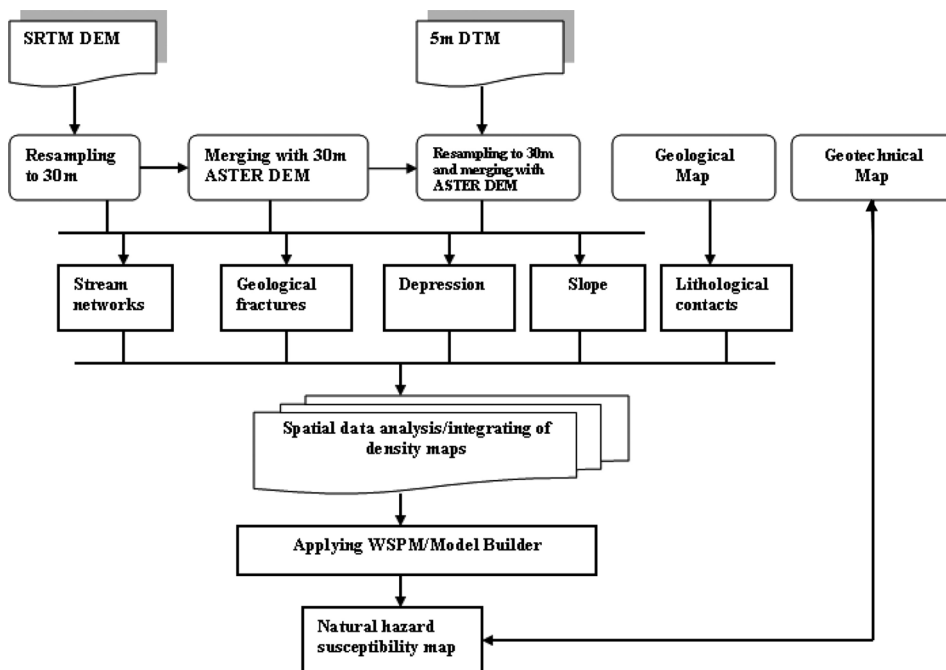


Figure 3. Flow chart of the methodology used for the study.

environment as input layers to perform the environmental prediction mapping (figure 3). The factors include: (i) geological fractures, which serve as channels and hence increase the rock weathering (ii) stream networks, which are often connected with geological fractures (Gerasimov and Korzhuev 1979, Ollier 1981), and hence, increases mechanical weathering, karst features development, (iii) depressions, which reflect high geological fractures intersections, karst features development and hence probability occurrence of environmental and geotechnical engineering problems, (iv) lithological contact and/or discontinuity between Kuala Limestone and Kenny Formation and granite, which can serve as passways for downward transport of rainwater to Kuala Lumpur Limestone bedrock and increase dissolution and probability of sinkholes and earth subsidence (Gue and Tan 2001) and (v) slope, which controls the speed of rivers, mechanical erosion was considered as a crucial factor in predicting flood and landslides occurrences.

3.2.1.1 Extraction of geological fractures. Geological fractures generally control relief, spatial distribution of stream network, and rock erosion under the influence of gravity (Young 1972, Gerrard 1981). Geological fracture intersections and looseness are the most important features of the Earth crust's increased seismicity, sinkholes and earth subsidence (Gelfand *et al.* 1972, Karakhanyan 1981, Korobeynik *et al.* 1982, Poletae 1992). Therefore, zones of geological fracture intersection, wetness and erosion can coincide with sites of landslide, sinkholes and earth subsidence (Karakhanyan 1981).

To carry out geological fractures crosscutting the entire study area, two modified techniques were applied. In the first technique, a DEM was used to calculate slope and aspect slope. After that, the calculated slope and aspect slope maps were enhanced by applying contrast stretching. In the second approach, a set of shaded relief in all directions (0° , 45° , ... 315°) with 28 times exaggeration in the Z dimension (Jordan and Csillag 2001) was calculated. The calculated maps were then enhanced by applying Sobel filter with 10% threshold followed by equalization histogram to facilitate the visual interpretation (Samy *et al.* 2011a). The visual interpretation based on the change of slope in the slope map and the change of the tone of the shaded relief was used to carry out the geological fractures.

Since the detection of linear features is partially dependent on the origin of a light source, the geological fractures extracted from different shaded relief maps were then overlaid in one layer in GIS environment to construct map of the extracted surface and subsurface geological fractures.

To spatially analyse the relationship of geological fractures to landslides, sinkholes and earth subsidence, maps of geological fractures' density and distance from geological fractures were prepared. The map was categorized into four classes from very low to very high. The map (layer) was given a weight 0.4 and the map classes were given rate of effectiveness (E) ranges from 35 to 5 in weighted spatial probability modelling. (tables 1 and 2).

3.2.1.2 Extraction of stream network. A D8 flow routing based on the 8-cell neighbourhood approach (Jenson and Domingue 1988) was used to automatically extract flow direction grid, and then, the major drainage network was delineated through a flow accumulation function, and specified by a threshold value of 30 cells. After that, the stream order and basins were delineated. The resulting stream network density map was categorized into four classes. These classes are very high susceptibility, high susceptibility, moderate susceptibility and low susceptibility. This map was assigned a weight of 0.35 in the weighted spatial probability modelling (tables 1 and 2).

Table 1. Ranks and weights for factors and their influencing classes used for sinkholes and earth subsidence susceptibility mapping.

Hazard factor	Probability classes	Average rank (R_f)	Weight (W_f)	Rate of effectiveness (E)
Geological fractures	I (very high)	87.5	40% (0.4)	35
	II (High)	62.5		25
	III (moderate)	37.5		15
	IV (low)	12.5		5
Stream network	I (very high)	87.5	35% (0.35)	30.6
	II (High)	62.5		21.8
	III (moderate)	37.5		13.1
	IV (low)	12.5		4.3
Micro-depressions	I (very high)	87.5	15% (0.15)	13.1
	II (High)	62.5		9.3
	III (moderate)	37.5		5.6
	IV (low)	12.5		1.8
Lithological contacts	I (very high)	87.5	10% (0.10)	8.7
	II (High)	62.5		6.2
	III (moderate)	37.5		3.7
	IV (low)	12.5		1.2

Table 2. Ranks and weights for factors and their influencing classes used for landslides and rock fall subsidence susceptibility mapping.

Hazard factor	Probability classes	Average rank (R_f)	Weight (W_f)	Rate of effectiveness (E)
Stream network	I (very high)	87.5	40% (0.4)	35
	II (High)	62.5		25
	III (moderate)	37.5		15
	IV (low)	12.5		5
Geological fractures	I (very high)	87.5	35% (0.35)	30.6
	II (High)	62.5		21.8
	III (moderate)	37.5		13.1
	IV (low)	12.5		4.3
Slope	I (very high)	87.5	15% (0.15)	13.1
	II (High)	62.5		9.3
	III (moderate)	37.5		5.6
	IV (low)	12.5		1.8
Depressions	I (very high)	87.5	10% (0.10)	8.7
	II (High)	62.5		6.2
	III (moderate)	37.5		3.7
	IV (low)	12.5		1.2

3.2.1.3 *Extraction micro-depressions.* For micro-depressions and pits extraction, Wood's method (1996) was used. A moving window size (3×3) is fitted to the DEM and the rate of change in gradient of a central pixel in relation to its neighbours is derived by a bivariate quadratic function.

Wood (1996) measured slope, minimum curvature and maximum curvature as a set to recognize morphometric features. These features can be identified using a set of

rules and criteria (Wood 1996). For example, pits and micro-depressions have negative values (<0) for minimum curvature. Finally, the density of micro-depressions was assigned of 0.15 and 0.10 in the weighted spatial probability modelling (tables 1 and 2). The map was assigned to four classes as: very high susceptibility, high susceptibility, moderate susceptibility and low susceptibility.

3.2.1.4 Delineation of lithological contacts. The lithological contacts can be defined as a boundary and/or discontinuity between different lithological units. The lithological contact between Kenny Hill Formation (met-sediments) and Kuala Lumpur Limestone serves as passways for downward transport of rainwater into Kuala Lumpur Limestone bedrock and increases its dissolution, thus there is high probability of occurrence of earth subsidence and sinkholes. So, it is important to include lithological contacts in natural hazard susceptibility analysis and modelling.

To delineate the lithological contacts, the geological map (figure 1(b)), and slope and curvature maps were used. The abrupt change in slope and curvature maps was used to delineate lithological contacts between Kuala Lumpur Limestone and Kenny Hill and granite using visual screen digitizing. Finally, the density of lithological contact was assigned as 0.10 in the weighted spatial probability modelling (table 1). The map was assigned to four classes: very high susceptibility, high susceptibility, moderate susceptibility, low and very low susceptibility.

3.2.1.5 Calculation of slope. Slope can be defined as the rate of change in elevation and expressed in percentage or/and in degrees. Slope and slope direction (aspect) play vital role in both rock fall and landslide occurrences especially in tropical regions (Gue and Tan 2001, Tsaparas *et al.* 2002). Slopes play a very strong role in determining rain water infiltration and acceleration as well as rock erosion and sediment accumulation (Subba *et al.* 2001). To highlight on this role, slope map was calculated from DEM. Slope map was assigned a weight of 0.15 in the weighted spatial probability modelling (table 1).

The aforementioned geomorphometric features and parameters were chosen based on their ability to provide meaningful insight into geomorphological and geological processes. Finally, the locations of buried ex-open pit mining ponds (previous mining activity) were digitized in polygons from archive topographic and geotechnical maps for the areas underlain by Kuala Lumpur Limestone bedrock.

3.2.2 Weighted Spatial Probability Modelling (WSPM). The Weighted Spatial Probability Modelling (WSPM) was applied to the map and landslide susceptibility was estimated using four essential GIS thematic maps extracted from remotely sensed data. Following a prior acknowledge and the previous other works in geotechnical probability modelling (Samy *et al.* 2010a), and groundwater potentiality mapping (i.e. Das 2000, Elewa and Qaddah 2011), the four essential thematic maps were ranked and re-ranked according to their level of contribution to environmental and geotechnical engineering problems occurrence. Therefore, they were classified from high to low contribution, and the same classes were used in the probability maps (tables 1 and 2). For instance, the factors of stream network and geological fractures are more effective to the landslide occurrence than depressions in areas of Kenny Hill Formation. Based on their level of contribution to sinkholes and earth subsidence occurrences, the integrated factors were given the following weights: geological fractures (40%), streams (35%), depression (15%) and

lithological contact (10%), and then the classes were categorized as high probability, moderate probability and low probability.

For sinkholes and earth subsidence, the ranks of four classes were classified as 100–75%, 75–50%, 50–25%, and 25–0%. Thus, the average ranks (R_f) of four classes were classified as 87.5, 62.5, 37.5 and 12.5% for classes from I to V, respectively (tables 1 and 2).

To determine the level of spatial association between the location of known landslides, earth subsidence and river flooding, the rate of effectiveness or significance contribution (E) for each factor (thematic map) was calculated using equation (1). For instance, if the weight of geological fractures equals 40%, and this is multiplied by the average rank of 87.5 (class I), the rate of effectiveness will be:

$$E = W_f \times R_f = 0.4 \times 87.5 = 35 \quad (1)$$

where W_f is the weight of each factor and R_f is the average rank of each factor.

Following equation (1) enables estimation of the rate of effectiveness to the natural hazards occurrence of each factor (layer). It also provides a relative analysis between various input layers. For WSPM, the various layers were overlaid and spatially analysed in GIS environment. Finally, the obtained susceptibility map was checked against the geotechnical map of Kuala Lumpur (GSM 2001).

It is important to note that, the ranking and calculated weights using WSPM were chosen based on the factors' (thematic maps) magnitudes and contributions to natural hazards occurrence. For example, the geological fractures, stream networks, depressions and lithological contacts showed the highest weight in the areas underlain by Kuala Lumpur Limestone, sinkholes and earth subsidence, while the stream networks, geological fractures and slopes exhibited the highest weight in the mountainous area of Kenny Hill Formation where landslides and rock fall occurred (tables 1 and 2).

3.2.3 Validation method. The result of susceptibility analysis and geohazard map were validated using locations of landslides, earth subsidence and sinkholes reported in the geotechnical map (GSM 2001).

As a first step of validation method, the natural hazard map (raster) was vectorized to points (predictor points). Then, terrain parameters [particularly relief (m), minimum curvature (1/100 m), maximum curvature (1/100 m), and slope percentage] for each point (both reported and predicted) were calculated (Samy *et al.* 2011b).

Validation of the WSPM and natural hazard map was performed by correlating mean, maximum, minimum and standard deviation of known landslides, sinkholes and earth subsidence with the produced susceptibility map. In addition, terrain parameters for each location of known and predicted landslides, cavities and earth subsidence were correlated.

4. Result and discussion

4.1 Geological fractures and natural hazard occurrence

The map of geological fractures extracted from DEM using the modified methods is shown in figure 5(a). The map shows distribution of the azimuths of the geological

fractures. Their orientations were commonly found to be in the NE–SW, NNE–SSW and WNW–ESE directions.

Sites of geological fracture intersections very closely associate with landslides, earth subsidence and sinkhole occurrence: the weight and rate of effectiveness are 0.4 and 35, respectively. This is a normal result substantiating facts that fault intersections often associate with landslides, sinkholes and earth subsidence occurrence and (Poletaev 1992, Florinsky 1993).

When a landslide inventory map was compared with density of geological fractures map, there is an indication that the geological fractures are affecting the susceptibility of Kuala Lumpur Limestone and Kenny Hill formations. The very high density of geological fractures within distance of 100 m of geological fractures exceeded the average landslides, earth subsidence and sinkholes' density of Kuala Lumpur areas (figure 4(a)). As the density of geological fractures increases, the probability of landslide occurrence increases and vice versa (figure 5(a)).

4.2 Stream network and natural hazard occurrence

The map of stream network extracted from DEM using D8 algorithm is shown in figure 5(a). According to stream network map, four major trendings characterize the study area: (i) NNE–SSW, (ii) WNW–ESE, (iii) NW–SE and (iv) NE–SW. These features are often connected with geological fractures and share similar trending. From this relationship, an indication can be obtained of the direction of geological fractures expected in the Kuala Lumpur Limestone, the direction in which karst is likely to be readily developed and hence the occurrence of earth subsidence and sinkholes (Zabidi *et al.* 2006).

Based on stream network, the locations nearer to the stream network (figures 4(b) and 5(b)) are the more susceptible areas to landslides, earth subsidence and sinkholes: the weight and rate of effectiveness are 0.35 and 30.6, respectively (tables 1 and 2).

4.3 Micro-depressions and natural hazard occurrence

The maps of micro-depressions and density of micro-depressions calculated from DEM are shown in (figures 4(c) and 5(c)). Micro-depressions affect surface rainwater movement, flow accumulation and soil moisture (Fedoseev 1959). The landslide, earth subsidence and sinkholes distribution was compared with density within each classes of micro-depression delineated. Results of data analysis show an increase in frequency of landslide, earth subsidence and sinkholes with increased density of micro-depressions. This is a normal result substantiating the fact that micro-depression is often associated with fault intersections and landslides, sinkholes and earth subsidence occurrence (Poletaev 1992, Florinsky 1993, 2000). Sites of high density of micro-depressions are very closely associated with landslides, sinkholes and earth subsidence occurrence: the weight and rate of effective were 0.15 and 13.1, respectively.

4.4 Slope and natural hazard occurrence

Slope map calculated from DEM is shown in figure 7(a). The slope map comprises of five classes for the study area, where the average slope was 45° (77%).

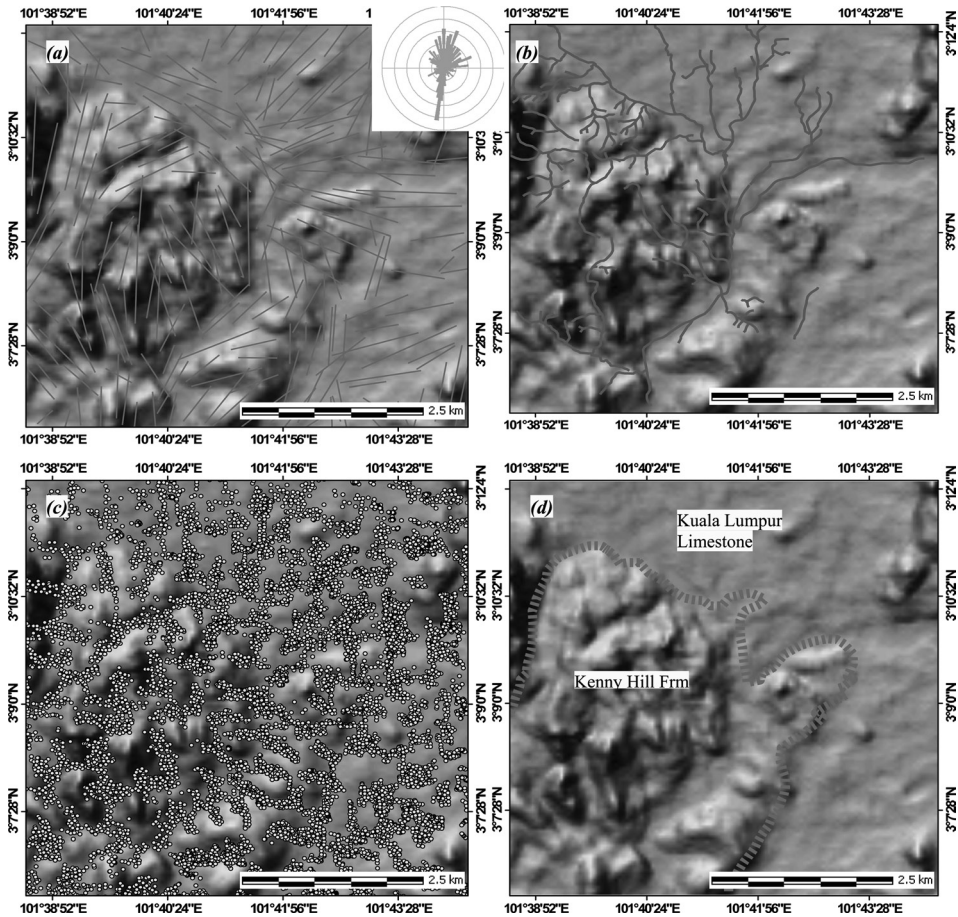


Figure 4. (a) Geological fractures map, (b) stream pattern map, (c) micro-depression map and (d) lithological contact. These were calculated from DEM.

In the mountainous areas of Kenny Hill Formation, there is water acceleration and active erosion in highly fractured rocks. This in turn will maximize the landslides and rock fall occurrence (Karakhanyan 1981, Tsaparas *et al.* 2002), because rain water saturation and infill sediments will be restricted to geological fracture intersections. Site at slope of 0–78, the rate of effectiveness is 1.8, has a very low probability of a landslide occurrence. Generally, elevation and slope show a symmetrical relationship with probability occurrence of landslides and rock fall, and asymmetrical relationship with probability occurrence of flooding (figures 6(b) and 7).

To highlight on the influence of slope on the occurrence of natural hazards, a comparative analysis was performed between mountainous areas of Kenny Hill Formation of steep slopes and relatively flat areas underlain by Kuala Lumpur Limestone (figure 8), and thus the following considerations must be taken into account. While in relatively gentle sloping terrain at lower elevation where the rivers decelerate, the river flooding, earth subsidence and sinkholes occur at depressions and regional fault zones intersections. Landslides and rock fall in mountainous areas of Kenny Hill formation was found to occur at higher elevation (> 70 m) and at

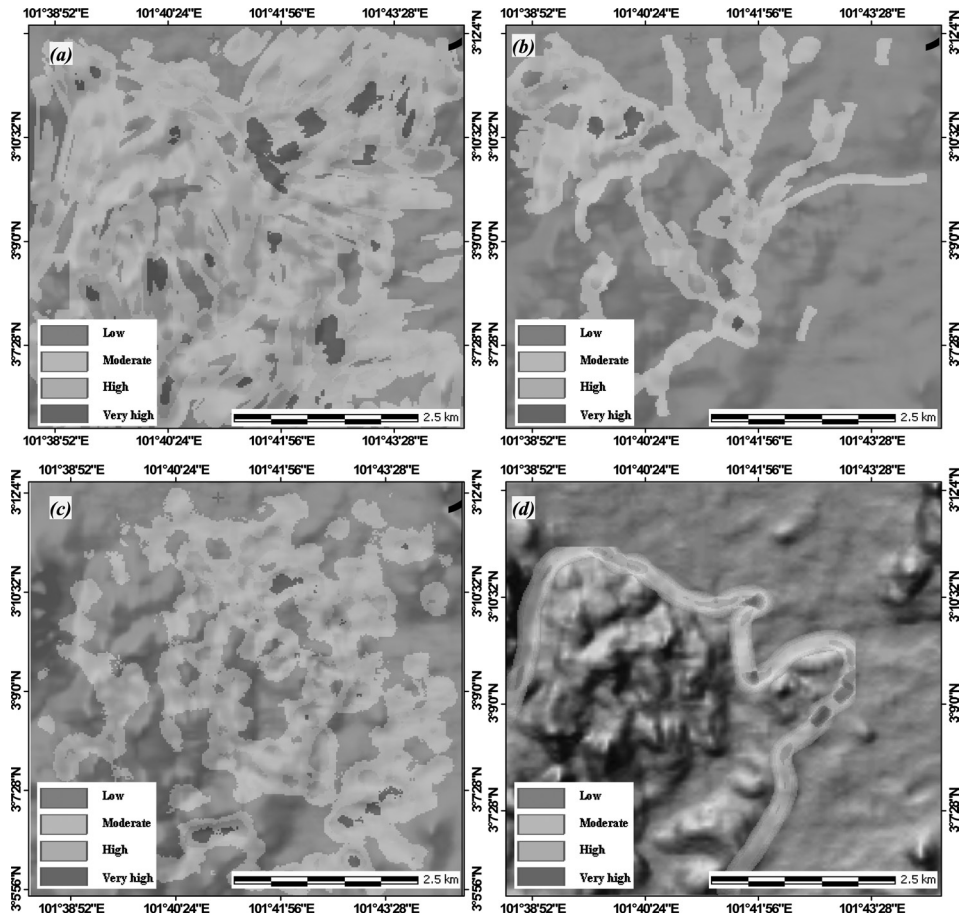


Figure 5. Density classes maps of (a) geological fractures, (b) micro-depressions, (c) stream networks and (d) lithological contacts for the study area. These were extracted from DEM using automated algorithm and visual interpretation.

steeper slopes ($>7^\circ$). The steeper slope directions in the E–W, NE–SW and NW–SE directions are the common directions in the mountainous areas (figure 7(a)). Sites at lower elevation of 0–42 m with a gentle slope of $0\text{--}7^\circ$ are closely correlated with river flooding, earth subsidence and sinkhole occurrence (figures 7(b)).

Results of data analysis show an increase in frequency of landslides with increased slope of up to 12° . After 12° , there is a sharp decrease in frequency of landslides. Further spatial analysis indicated that landslides, earth subsidence and sinkholes in weathered and highly fractured rocks have occurred at a lower slope angle of 7° than massive and hard rocks, especially when rainfall exceeds 500 mm. The frequency of landslides was compared with lithological map (figure 1(b)) and the density of landslides within each lithological unit was calculated. The mountainous area of Kenny Hill Formation (meta-sediments) is most susceptible to slope instability and deeply weathered with higher slopes and landslides. The Kuala Lumpur Limestone, as it is a highly fractured rock, already has zones of dissolution. Zones of dissolution of this rock make it susceptible to earth subsidence and sinkholes, particularly where it forms extreme karst.

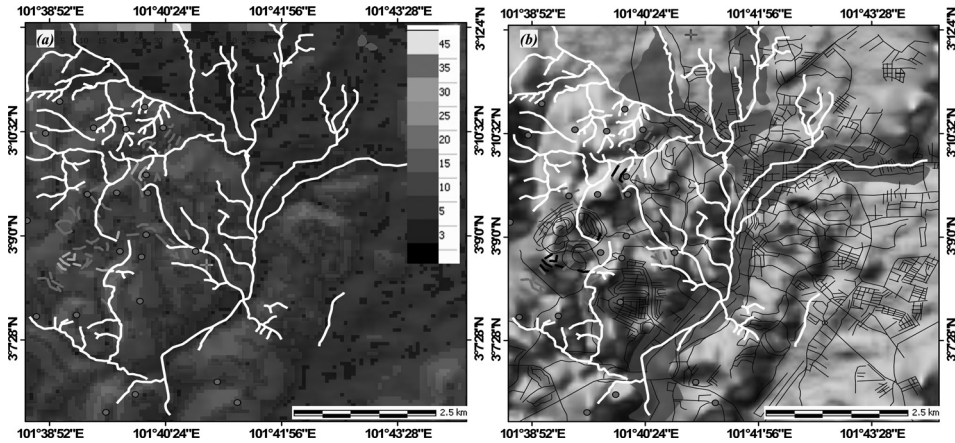


Figure 6. Major rivers and stream network are draped over (a) slope and (b) shaded relief maps calculated from DEM. The blue polygons highlight the areas at lower elevation of <41 m that having high flooding susceptibility. The red dots highlight the reported landslide locations and pink lines highlight the rock fall potential locations.

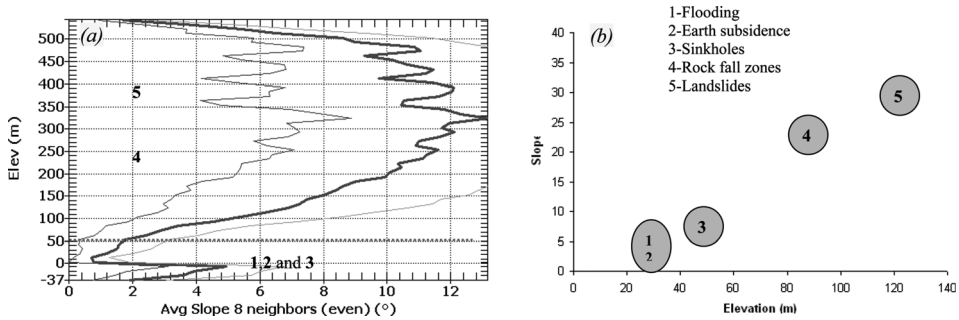


Figure 7. (a) Slope versus elevation diagram of the study area and (b) profile of morphometric parameters. These show that the geohazard occurrence is topographically controlled.

4.5 Lithological contact and natural hazard occurrence

Figures 4d and 5d show the maps of lithological contact and density of lithological contact between Kuala Lumpur Limestone and Kenny Hill Formation. This lithological contact serves as an underground channel for groundwater movement and increases the probability occurrence of earth subsidence and sink holes (Gue and Tan 2001). Spatial distribution of earth subsidences and sinkholes was compared with density within each class of lithological contact in Kuala Lumpur Limestone and Kenny Hill Formation and granite. Results indicated that sinkholes and earth subsidence frequency increases gradually with a decrease in distance from lithological contact. Spatial analysis shows that 90% of known earth subsidence and sinkholes are located within 50 m of lithological contacts: the weight and rate of effective are 0.1 and 8.7, respectively. Further spatial data analysis indicated that earth subsidence and sinkholes on lithological contact occurred at lower angle, compared with other locations. Several geotechnical engineering problems related to lithological contact

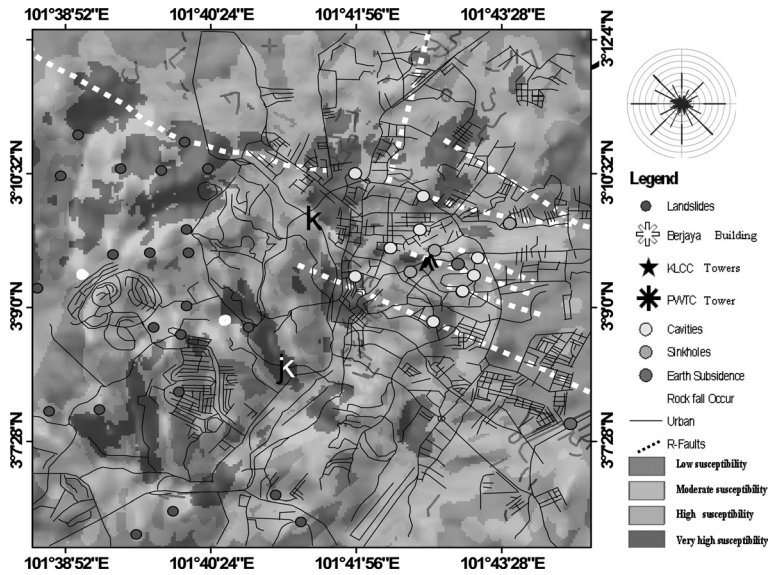


Figure 8. Geohazard susceptibility map of the Kuala Lumpur city centre.

have occurred during construction of Pan Pacific Hotel and Putra World Trade Center (PWTC) (Azam *et al.* 1996, Gue and Tan 2001).

5. Weighted Spatial Probability Modelling (WSPM) and validation

The obtained natural hazards susceptibility map pointed out that the high probability locations of sinkholes and earth subsidence are almost located in the areas where geological fractures intersected, which often are situated in the depressions and lithological contacts in the central part of Kuala Lumpur (figure 8).

The areas having very high and high probability occurrence of flooding exhibit an area of 17.116 km² (32.95%). The high flooding susceptibility class occupies 11.9 km² (22.9%), while the moderate susceptibility class occupies 19.4 km² (37.5%) of the map, indicating the overall low and moderate natural hazard susceptibility of the Kuala Lumpur city centre. These areas are Baharu, Medan Tuanku, Brickfields, Park Avenue Homes and Haji Abdullah Counties (figure 6(b)).

The high probability localities for landslides and rock fall occurrence are almost located in areas where the slope ($>7^\circ$) is steep with intensive stream networks and elevation of 70 m. The areas having very high natural hazard susceptibility show an area of 4.1 km² (8 %), whereas the areas characterized by low susceptibility for occurrence of natural hazards occupy approximately 16.4 km² (31.6%) of total Kuala Lumpur area (figure 8 and table 3).

Overlaying of locations of known landslides, earth subsidence and sinkholes and the constructed natural hazard map is shown in figure 8. Commonly, sinkholes and earth subsidence occurred in the flat areas (0–7%), while landslides occurred in undulating areas (7–15%). It can be seen from figure 8 that very high and high susceptible classes of sinkholes are located in areas of high density classes of geological fractures, lithological contact and stream network.

Table 3. Areas of geohazard map classes (km²). Total area studied: 51.943 km².

Potential class	Very high	High	Moderate	Low
Area (km ²)	4.155	11.907	19.487	16.394
Area (% of Kuala Lumpur city center area)	7.9	22.9	37.5	31.6

Based on visual inspection, the very high susceptibility class is in general agreement with the spatial distribution of reported landslides, earth subsidence and sinkholes within the area investigated. High and very high classes of flood, earth subsidence and sinkholes are closely associated with low-lying ($<7^\circ$), where Kuala Lumpur are present. High and very high classes of landslides are closely associated with mountainous areas ($>7^\circ$), where Kenny Hill Formation is present. The validation of natural hazards susceptibility map was measured. The spatial distribution of landslides in various susceptibility classes increases as the degree of landslide susceptibility increases.

From the comparison of geotechnical engineering map and natural hazards susceptibility map. The locations of known landslides, earth subsidence and sinkholes are coinciding in many locations, in spite of difference in spatial resolution (pixel size) and terrain attributes. In reality, cavities, sinkholes and earth subsidence that reported in the published geotechnical engineering (GSM 2001) were observed within the high density of the extracted geological fractures, stream network lithological contacts and depressions, and in areas underlain by Kuala Lumpur Limestone bedrock rather than throughout. However, landslides and rockfall occurrence were observed in mountainous areas of Kenny Hill Formation (meta-sediments) with steeper slopes rather than areas under by Kuala Lumpur Limestone.

Natural hazard susceptibility analysis result was validated using locations of landslides, sinkholes and earth subsidence that were reported in the geotechnical map (GSM 2001).

Validation was performed by correlating the moment statistics and terrain parameter values [particularly mean and standard deviation, slope (%), relief (m) and minimum and maximum curvature (1/100 m)] of the reported landslides, sinkholes and earth subsidence locations with the natural hazard susceptibility map (Samy *et al.* 2011b).

Terrain parameters of each known and predicted point of landslides, earth subsidence and sinkholes and their statistics for maximum, minimum, mean and standard deviation are shown in figure 9 and table 4. The locations of predicted natural hazards have mean and standard deviation of 151 and 50, respectively, while the locations of known natural hazards have mean and standard deviation of 148 and 49, respectively (figure 9(a)). The peaks and trough of the terrain parameters graphs (figure 9(b–e)) show strong agreement with little difference in values between predicted and known locations of earth subsidence, sinkholes and landslides. Variations in the terrain parameter values of predicted and known locations are attributed to the difference in spatial resolution of the remote sensing and ancillary data.

Results obtained in this study demonstrate that the WSPM not only provides precise mapping and predicting of natural hazard susceptibility but also enhances the applicability of remote sensing and GIS to spatial-related computation. The resultant natural hazard susceptibility map permits better understanding of geohazard setting of the area underlain by Kuala Lumpur Limestone and the adjacent mountainous areas.

Table 4. (Continued).

Terrain parameters of reported natural hazard (reported points)				Terrain parameters of predicted natural hazard (predicted points)			
Lat.(N)	Long. (E)	Slope (%)	Relief (m)	Lat.(N)	Long. (E)	SLOPE (%)	RELIEF(m)
3.14626	101.6799	17.97	43	3.155432	101.699	14.99	42
3.146258	101.68	17.97	43	3.161371	101.705	15.99	45
3.144682	101.6681	17.93	45	3.171115	101.7107	16.99	47
3.133823	101.6677	12.64	15	3.176437	101.6986	12.93	10
3.130436	101.6536	8.43	53	3.164634	101.7103	5.99	47
3.130029	101.6447	8.43	40	3.165852	101.7257	8.99	44
3.127985	101.7369	5.99	37	3.161331	101.7124	6.82	35
3.114159	101.6849	11.93	53	3.157134	101.7085	9.86	57

Lat. = altitude; Long. = Longitude; Maxic = maximum curvature in (1/100 m); Minic = minimum curvature in (1/100 m).

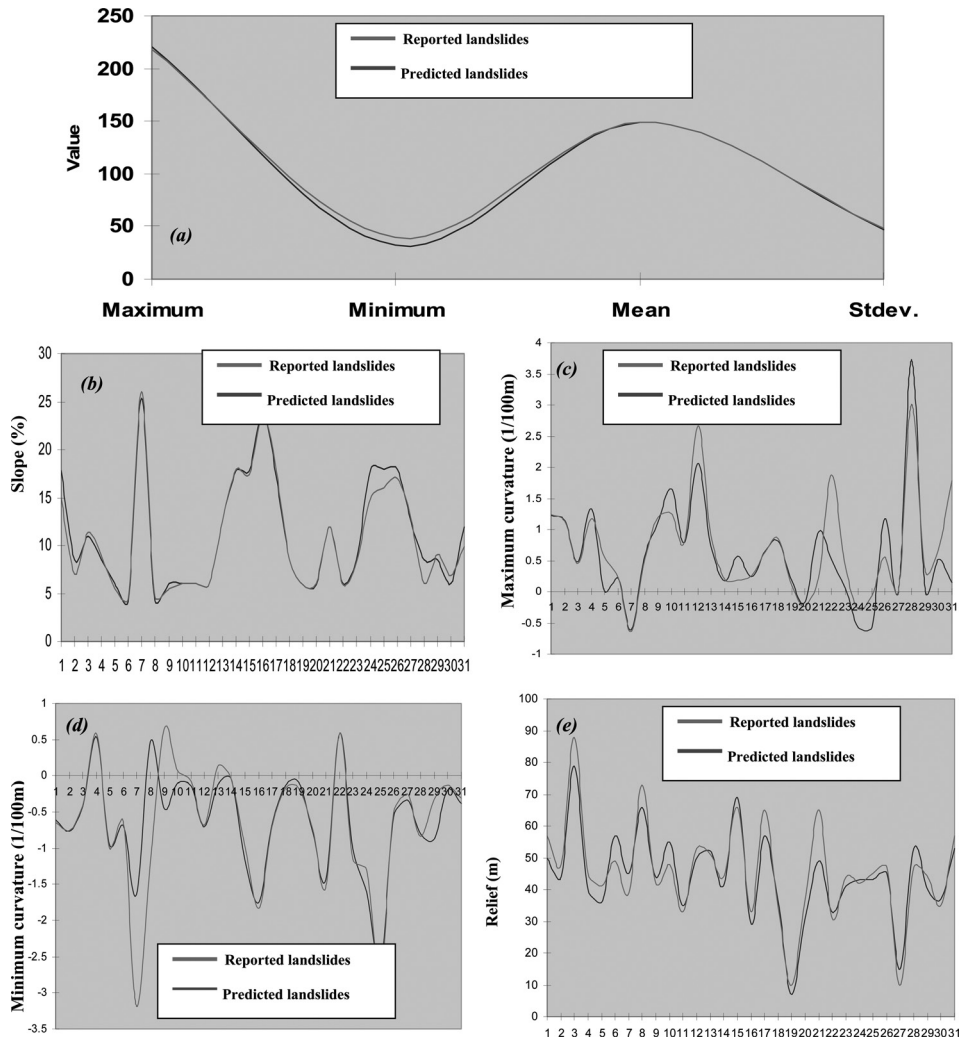


Figure 9. Graphs of basic statistics and terrain parameters (surface morphometric signatures) of sinkholes, cavities and earth subsidence that were reported in geotechnical (blue) and predicted (pink) maps. Available in colour online

Future work will involve real time model and the application of both SAR data (e.g. ALOSPALSAR L band), and Light Detection And Range (LiDAR) in order to construct more accurate slope and elevation maps, delineate more buried channels and fractured zones and their associated karst features underneath alluvial deposits and enable a better understanding of the geotechnical engineering and natural hazard setting of the city of Kuala Lumpur.

6. Conclusions

The current study represents a geohazard model approach to integrate the essential geological and geomorphological factors controlling environmental and geotechnical engineering problems, and thus to reveal the information in a predictor map

exhibiting spatial data for tropical areas with high response to the environmental and geotechnical engineering problems in Kuala Lumpur, Malaysia.

Five essential layers (factors) were extracted from 20 m spatial resolution DEM. These layers were geological fractures, stream networks, micro-depressions and lithological contacts. These layers were ranked and re-ranked using WSPM in GIS environment according to the rate of effectiveness of layers to the natural hazard occurrence. Hence, the hazard predictor map was validated by comparison with the published geotechnical engineering map of Kuala Lumpur, Malaysia and geophysical reports. It was found that the constructed map agrees well with the published maps and locations of reported landslides (GSM 2001).

This shows that the integrated approach outlined has its own advantages and can be effectively used in geotechnical and geohazard application. The resulting susceptibility map of Kuala Lumpur indicates that various locations have high probability for the occurrence of environmental and geotechnical engineering problems with significantly different magnitudes.

Several sites that are cross cut by geological fractures and stream network were predicted to have very high and high hazard through the constructed predictor map. These sites could be zones of cavities, rock dissolution and extreme karstification of the Kuala Lumpur Limestone bedrock and Kenny Hill Formation. The results obtained show that maps of WSPM can be used to predict the unpredictable environmental and geotechnical engineering problems in areas underlain by highly fractured carbonate bedrocks.

References

- AZAM, T., HASHIM, H. and IBRAHIM, R., 1996, Foundation design for Petronas Twin Towers at Kuala Lumpur City Center. In *12th SEGAGC*, 6–19, Kuala Lumpur, pp. 485–492.
- CHOW, W.S., MIOR, S., MIOR, J., SAZALI, Y., 1996a, Geological and geomorphological investigations of debris flow at Genting Sempah, Selangor. In *Proceedings of GSM Forum on Geohazards: Landslide & Subsidence*, Kuala Lumpur, 22 October 1996, *Geological Society of Malaysia*, pp. 5.1-5.15.
- DAS, D., 2000, GIS application in hydrogeological studies. Available online at: www.gisdevelopment.net. (accessed August 2009.)
- ELEWA, H.H., and QADDAH A.A., 2011, Groundwater potentiality mapping in the Sinai Peninsula, Egypt, using remote sensing and GIS-watershed-based modeling. *Hydrogeology Journal*, DOI 10.1007/s10040-011-0703-8.
- FEDOSEEV, A.P., 1959, Soil moisture and terrain topography. In *Agricultural Meteorology*, KONYUKHOV, N.A. (Ed.), in Russian (Moscow: Hydrometeorological Press).
- FLORINSKY, I.V., 1993, Digital elevation model analysis for linear landsurface structure recognition. Abstract of Ph.D. thesis, Moscow State University of Geodesy and Cartography, Moscow, 17 pp., in Russian.
- FLORINSKY, I.V., 2000, Relationships between topographically expressed zones of flow accumulation and sites of fault intersection: analysis by means of digital terrain modelling. *Environmental Modelling and Software*, **15**, pp. 87–100.
- GELFAND, I.M., GUBERMAN, S.H.A., IZVEKOVA, M.A., KEILIS-BOROK, V.I., RANZMAN, E.JA., 1972, Criteria of high seismicity, determined by pattern recognition. *Tectonophysics*, **13**, pp. 415–422.
- GEOLOGICAL SURVEY MALAYSIA (GSM), 1995, Geological map of Peninsular Malaysia, scale 1:63360, Kuala Lumpur, New Series, sheet 94.

- GEOLOGICAL SURVEY MALAYSIA (GSM), 2001, Geotechnical map of Kuala Lumpur and surrounding areas, scale 1:25000, Wilayah Persekutuan Series L8010, Part of sheet 94a, 94b, 94d, 94e&94f, Published by digital process.
- GERASIMOV, I.P. and KORZHUEV, S.S. (Eds.), 1979, *Morphostructural Analysis of the Drainage Network of the USSR*. Moscow: Nauka, 304 pp., in Russian.
- GERRARD, A.J., 1981, Soils and Landforms. An Integration of Geomorphology and Pedology. London: George Allen and Unwin, 219 pp.
- GOBBET, D.J., 1964, The lower paleozoic rocks of Kuala Lumpur, Malaysia. *Federation Museum's Journal*, **9**, pp. 67–79
- GUE, S.S. and TAN, Y.C., 2001, The foundation system for Berjaya Times Square. Seminar on Mega Projects: A Study on Civil Engineering Projects, University Technology Malaysia, Johor Bharu, Malaysia.
- HENGL, T., DAVID, G., ROSSITER, F., 2003, Supervised landform classification to enhance and replace photo-interpretation in semi-detailed soil survey. *Soil Science Society of America Journal*, **67**, pp. 1810–1822.
- JENSON, S.K. and DOMINGUE, J.O., 1988, Extracting topographic structure from digital elevation data for geographic information system analysis. *Photogrammetric Engineering and Remote Sensing*, **54**, pp. 1593–1600.
- JORDAN, G. and CSILLAG, G., 2001, Digital terrain modelling for morphotectonic analysis: A GIS framework. In *DEMS and geomorphology*, H. Ohmori (Ed.), Vol. **1**, pp. 60–61 (Tokyo: Nihon University) Special Publication of the Geographic Information Systems Association.
- KARAKHANYAN, A.S., 1981, Recognition of amply-dimensional landslides and rock blocks torn and slipped down by gravity with the use of remotely sensed data. *Izvestiya Vysshikh Uchebnykh Zavedeny, Geologiya i Razvedka*, **3**, pp. 130–131 in Russian.
- KOROBENNIK, V.M., KOMAROVA, M.V. and SHTENGELOV, Y.E., 1982, Permeable- faults of the earth crust in the Crimea and the north-western Black Sea area. *Doklady Akademii Nauk Ukrainskoi SSR, Series B*, **2**, pp. 13–16, in Russian with English abstract.
- MAH, A., TAYLOR, G.R., LENNOX, P. and BALIA, L., 1995, Lineament analysis of Landsat thematic mapper images, Northern Territory, Australia. *Photogrammetric Engineering and Remote Sensing*, **61**, pp. 761–773.
- OLLIER, C.D., 1981, *Tectonics and Landforms. Geomorphology Texts*, 6. New York: Longman Group Limited, 324 pp.
- POLETAEV, A.I., 1992, *Fault Intersections of the Earth Crust* (Moscow: Geoinformmark), 50 pp., in Russian.
- SAMY, I.E., 2006, Remote sensing for hydrological application in the vicinity of Al Dhied, UAE. MSc, University Technology Malaysia (UTM), Malaysia.
- SAMY, I.E., SHATTRI, M., AHMED, R.M., BUJANG, B.K., 2010a, Geotechnical modeling of fractures and cavities that are associated with geotechnical engineering problems in Kuala Lumpur limestone, Malaysia, *Environmental Earth Sciences*. DOI 10.1007/s12665-010-0497-3.
- SAMY, I.E., SHATTRI, M., BUJANG, B.K., AHMAD, R.M., 2010b, Topographic openness algorithm for characterizing geologic fractures of Kuala Lumpur limestone bedrock using DEM. *Journal of Geomatics*, **4**, pp. 60–68.
- SAMY, I., SHATTRI, M., BUJANG, B.K., AHMAD, R.M., 2011a, Application of terrain analysis to the mapping and spatial pattern analysis of subsurface geological fractures of Kuala Lumpur limestone bedrock, Malaysia. *International Journal of Remote Sensing*, **33**, pp. 3176–3196.
- SAMY, I., SHATTRI, M., BUJANG, B.K., AHMAD, R.M., 2011b, Structural geology control the limestone bedrock that associated with piling problems using remote sensing and GIS: a modified geomorphology method. *Environmental Earth Science Journal*. DOI:10.1007/s12665-011-1440-y
- STAUFFER, P.H., 1968, The Kuala Lumpur fault zone: a proposed major strike-slip fault across Malaya. *Newsletter Geological Society Malaysia*, **15**, pp. 2–4.

- SUBBA, R.N, CHAKRADHAR, G.K.J., SRINIVAS, V., 2001, Identification of groundwater potential zones using remote sensing techniques in and around Guntur Town, Andhra Pradesh, India. *Journal of the Indian Society of Remote Sensing*, **29**, pp. 69–78.
- TAN, B.K., 1987, Geology and urban development of Kuala Lumpur, Malaysia. In *Proceedings of LANDPLAN III Symposium*, December 1986, Hong Kong (Hong Kong: Association of Geoscientists for International Development), pp. 127–140.
- TAN, B.K., 1996, Project KLCC: geology, soils and foundations. *Warta Geology*, **22**, pp. 73–74.
- TSAPARAS, I., RAHARDJO, H., TOLL, D.G., LEONG, E.C., 2002, Controlling parameters for rainfall-induced landslides. *Computers and Geotechnics*, **29**, pp. 1–27.
- WOOD, J.O. 1996, The geomorphological characterization of digital elevation models, PhD thesis, University of Leicester, Department of Geography, Leicester, UK.
- XEIDAKIS, G.S., TOROK, S., SKIAS and KLEB, B. 2004, Engineering geological problems associated with karst terrains: Their investigation, monitoring, and mitigation and design of engineering structures on karst terrains. *Bulletin of the Geological Society of Greece*, **XXXVI**, pp. 1932–1941.
- YEAP, E.B., 1987, Engineering geological site investigation of former mining areas for urban development in Peninsular Malaysia. *Geological Society of Hong Kong Bulletin*, **3**, pp. 319–334.
- YOUNG, A., 1972, *Slopes*. Edinburgh: Oliver and Boyd, 288 pp.
- ZABIDI, H., HENRY, M. and DE FREITAS, M.H., 2006, Structural studies for the prediction of karst In the Kuala Lumpur limestone, *Journal of the Geological Society of London* 2006 IAEG2006, Paper number 264.